HOKKAIDO UNIVERSITY

Title	Effects of Snow and Remineralization Processes on Nutrient Distributions in Multi-Year Antarctic Landfast Sea Ice
Author(s)	Sahashi, Reishi; Nomura, Daiki; Toyota, Takenobu et al.
Citation	Journal of Geophysical Research Oceans, 127(7), e2021JC018371 https://doi.org/10.1029/2021JC018371
Issue Date	2022-07-01
Doc URL	https://hdl.handle.net/2115/87739
Rights	Copyright 2022. American Geophysical Union.
Type	journal article
File Information	JGR Oceans 2022 Sahashi.pdf

Hokkaido University Collection of Scholarly and Academic Papers : HUSCAP

Check for updates

JGR Oceans

RESEARCH ARTICLE
10.1029/2021JC018371

Effects of Snow and Remineralization Processes on Nutrient Distributions in Multi-Year Antarctic Landfast Sea Ice

Reishi Sahashi[1], Daiki Nomura[1,2,3], Takenobu Toyota[4], Manami Tozawa[1], Masato Ito[5], Pat Wongpan[4,6,7], Kazuya Ono[4], Daisuke Simizu[5], Kazuhiro Naoki[8], Yuichi Nosaka[9], Takeshi Tamura[5,10], Shigeru Aoki[4], and Shuki Ushio[5,10]

[1]Faculty of Fisheries Sciences, Hokkaido University, Hakodate, Japan, [2]Field Science Center for Northern Biosphere, Hokkaido University, Hakodate, Japan, [3]Arctic Research Center, Hokkaido University, Sapporo, Japan, [4]Institute of Low Temperature Science, Hokkaido University, Sapporo, Japan, [5]National Institute of Polar Research, Tachikawa, Japan, [6]Institute for Marine and Antarctic Studies, University of Tasmania, Hobart, Australia, [7]JSPS International Research Fellow, Japan Society for the Promotion of Science, Tokyo, Japan, [8]Research and Information Center, Tokai University, Tokyo, Japan, [9]School of Biological Sciences, Tokai University, Sapporo, Japan, [10]Graduate University for Advanced Studies (SOKENDAI), Tachikawa, Japan

Abstract We elucidated the effects of snow and remineralization processes on nutrient distributions in multi-year landfast sea ice (fast ice) in Lützow-Holm Bay, East Antarctica. Based on sea-ice salinity, oxygen isotopic ratios, and thin section analyses, we found that the multi-year fast ice grew upward due to the year-by-year accumulation of snow. Compared to ice of seawater origin, nutrient concentrations in shallow fast ice were low due to replacement by clean and fresh snow. In deeper ice of seawater origin (the lower half of the multi-year fast ice column), remineralization was dominated by the degradation of organic matter. By comparison between first- and muti-year ice, the biological uptake and the remineralization were dominated in relatively young ice and older ice, respectively, under the physical process of brine drainage.

Plain Language Summary Multi-year landfast sea ice (fast ice) is abundant around the coast of Antarctica. Fast ice is an important component of Antarctic coastal marine ecosystems, providing a prolific habitat for ice algal communities. Although nutrients are essential for biological productivity within sea ice, the status of nutrients and processes affecting nutrient concentrations were previously not known for multi-year fast ice. Here, we collected sea-ice cores from multi-year fast ice in Lützow-Holm Bay, East Antarctica, and we analyzed nutrient concentrations using physical and biogeochemical parameters. Nutrient concentrations in the upper parts of the sea ice decreased due to the accumulation of clean (nutrient-free) snow through melting and refreezing processes, contributing to upward ice growth. In deeper parts of the sea ice, nutrient concentrations were greatly affected by biological processes such as remineralization during the degradation of organic matter within sea ice.

Key Points:

- Antarctic multi-year landfast ice grew upward due to the year-by-year accumulation of snow
- Nutrient concentrations decreased in the upper sea ice due to the replacement by clean snow
- In deeper sea ice, remineralization by degradation of organic matter drove nutrient concentrations

Supporting Information:

Supporting Information may be found in the online version of this article.

Correspondence to:

D. Nomura,
daiki.nomura@fish.hokudai.ac.jp

Citation:

Sahashi, R., Nomura, D., Toyota, T., Tozawa, M., Ito, M., Wongpan, P., et al. (2022). Effects of snow and remineralization processes on nutrient distributions in multi-year Antarctic landfast sea ice. *Journal of Geophysical Research: Oceans*, *127*, e2021JC018371. https://doi.org/10.1029/2021JC018371

Received 21 DEC 2021
Accepted 1 JUL 2022

Author Contributions:

Investigation: Pat Wongpan, Kazuya Ono, Daisuke Simizu, Kazuhiro Naoki, Yuichi Nosaka, Takeshi Tamura, Shuki Ushio
Writing – original draft: Takenobu Toyota, Manami Tozawa, Pat Wongpan, Kazuya Ono, Takeshi Tamura

© 2022. American Geophysical Union. All Rights Reserved.

1. Introduction

Multi-year landfast ice (fast ice) is abundant around Syowa Station, Lützow-Holm Bay, East Antarctica (Fraser et al., 2012, 2021; Ushio, 2006). This region receives relatively abundant snowfall and high snow accumulation rates over sea ice (Toyota et al., 2016), forming ice of snow origin such as "snow ice" and "superimposed ice" (Kawamura et al., 1997; Nomura et al., 2012, 2018). In general, snow ice forms under the weight of overlying snow on the sea ice, which depresses the ice–snow interface to below sea level; the subsequent flow of seawater into the snow forms a flooded slush layer that then freezes (Maksym & Jeffries, 2000; Sturm & Massom, 2017). During summer, the snow surface melts in the sunlight and warmer temperatures; the snowmelt then infiltrates the slush layer, decreasing its salinity to well below that of seawater (Nomura et al., 2012, 2018). However, in Lützow-Holm Bay, ice thickening due to the formation of snow ice does not necessarily depress the sea ice–snow interface to below sea level. In this case, when the shallowest snow thaws, the snowmelt permeates the sea ice–snow interface below the freezing point and refreezes, forming superimposed ice (Kawamura et al., 1997; Nomura et al., 2018). The difference between these two types of ice is that snow ice forms from a mixture of snow and seawater, whereas superimposed ice forms only from snow. Due to the abundance of snow around Syowa Station, it is considered that superimposed ice forms only after sea ice stops sinking under the weight of overlying snow.

Because sea ice forms from seawater, the biogeochemical components in seawater are preserved in sea ice upon its formation. Various changes affect these biogeochemical components, particularly nutrients, after their entrapment in sea ice. For example, NO_3^-, NO_2^-, NH_4^+, and PO_4^{3-} are involved in biological activities such as photosynthesis and remineralization by microorganisms such as bacteria and phytoplankton, notably ice algae, microphytes inhabiting the bottom most layers of sea ice (Arrigo et al., 2010; Gleitz et al., 1995). Diatoms, which are considered to be the main primary producers in sea ice, also use $Si(OH)_4$ to form their frustules (Arrigo et al., 2010; Tréguer & De La Rocha, 2013). In addition to the consumption of nutrients by ice algae, high-salinity and high-nutrient brines are discharged beneath the sea ice over time (Fripiat et al., 2017). Nutrients are resupplied by remineralization during the degradation of organic matter within sea ice by heterotrophs and bacteria (Roukaerts et al., 2021; Thomas et al., 1995), as well as by convection through brine channels (Nomura et al., 2009; Vancoppenolle et al., 2010).

Primary production is also active in the nutrient-rich, seawater-flooded slush layer formed at the sea-ice surface during the formation of snow ice (Ackley & Sullivan, 1994; Fritsen et al., 1994; Kattner et al., 2004; Nomura et al., 2018; Schnack-Schiel et al., 2001). The snow cover on sea ice therefore plays an important role in increasing the productivity of the sea-ice surface (e.g., Saenz & Arrigo, 2014). When the slush freezes, it becomes snow ice, preserving the biogeochemical components (Kawamura et al., 1997; Nomura et al., 2018). However, the thick sea ice produced in areas receiving abundant snowfall prevents seawater from flowing along the sea-ice surface, limiting productivity; therefore, snow cover can only increase productivity in the slush layer by so much. Furthermore, whereas snow-free sea ice grows downward due to the freezing of seawater, snow-covered sea ice grows upward due to the formation of snow ice and superimposed ice, such that melting progresses from the bottom of the sea ice (Kawamura et al., 1997). Thus, snow cover greatly affects biogeochemical distributions and circulations in sea ice.

Fast ice plays a crucial role in the biogeochemical cycle and marine ecosystem functions of the Antarctic coast because it hosts well-established habitats (in terms of nutrients, temperature, salinity, and light) for stable primary production (Arrigo, 2017; Wongpan et al., 2018). Because primary production in sea ice promotes the proliferation of zooplankton, that is, secondary and higher producers, it is essential to know how the biogeochemical composition of fast ice changes. However, although many studies have explored nutrient changes in first-year fast ice (e.g., Lim et al., 2019), research remains limited on biogeochemical components in multi-year fast ice that has continued to grow year-by-year. Furthermore, of the few studies that have focused on nutrient dynamics in multi-year land-fast ice (Nomura et al., 2018), their sea-ice samples provide only single-year observations. Therefore, no study has rigorously investigated the processes of nutrient cycling in multi-year sea ice. Because multi-year fast ice has remained fixed to the coast for a long time (Fraser et al., 2012, 2021), it is ideal for examining the temporal evolution and interannual variation of nutrient concentrations and other biogeochemical parameters in a single location.

The Japanese Antarctic Research Expedition (JARE) has monitored the multi-year fast ice near Syowa Station in Lützow-Holm Bay for many years. In recent years, it has been reported that the multi-year fast ice in Lützow-Holm Bay periodically breaks up and flows out to sea (Aoki, 2017; Ushio, 2006). Because ice thickness reflects the strength of sea ice, sea-ice monitoring efforts have recently collected annual ice core samples from an easily accessible and stable area near Syowa Station, ideal samples for tracking year-to-year changes. Additionally, because new ice formed after the partial ice breaks up and outflows, it is possible to track the cycling of biogeochemical components through the ice by comparing early stages of sea-ice formation with the initial multi-year ice.

In this study, we analyzed multi-year fast ice near Syowa Station to evaluate the effects of snow and biological activity on the vertical distribution of nutrient concentrations in sea ice. We investigated the factors affecting nutrient concentrations in the multi-year fast ice by collecting and comparing nearby first-year ice. Specifically, based on annual sampling during the 56–60th JAREs (2015–2019), we analyzed: (a) the structure and formation process of ice using thin section photographs, salinity, and stable oxygen isotopic ratios ($\delta^{18}O$); (b) the vertical distribution of nutrient concentrations in the fast ice; (c) the influence of snow (based on snow fraction) on nutrient distributions; and (d) the cycling of nutrient concentrations due to biological activity within fast ice using sea-ice salinity, and nutrient concentrations as proxies.

2. Materials and Methods

2.1. Sampling and Sample Preparation

Sea ice observations of multi-year fast ice were performed during the summers (January and February) of 2015–2019 as part of the 56–60th JAREs (Figure 1, Table 1). Sea-ice cores were collected near Syowa Station. Ice cores were sampled using an ice corer (Geo Tecs Co., Ltd., Chiba, Japan) with an internal diameter of 0.09 m. Cores were immediately placed in tubular polyethylene bags and kept horizontal in a cooler box along with refrigerants to maintain below-freezing temperatures and minimize brine drainage from the core. Fresh snow samples were collected with an acid-washed polycarbonate shovel and placed into polyethylene zipper storage bags. For comparison, four cores of first-year fast ice were also collected (Table 1).

Note that in Table 1, only the top 2.78 and 2.47 m of ice were sampled for cores JARE58_KU3 and JARE59_2, respectively, because the ice was too thick to sample the entire column. As part of the ice monitoring at Syowa Station, an electromagnetic (EM) ice thickness survey was conducted near our coring site in January 2018; the ice thickness was approximately 6 m.

Under-ice water was collected through the coring holes with a Teflon water sampler (GL Science Inc., Japan) from 1 m below the bottom of the sea ice during JARE60 (2019). Water samples were collected approximately 30 min after the ice core at JARE60_KU2 was drilled to avoid potential artifacts associated with the disturbance of drilling. All collected water samples were subsampled into (a) a 120-mL glass vial (Maruemu Co., Ltd., Osaka, Japan) for salinity measurement, (b) a 15-mL glass screw-cap vial (Nichiden-Rika Glass Co. Ltd, Kobe, Japan) for $\delta^{18}O$ analysis, (c) a 10-mL polyethylene screw-cap vial (Eiken Chemical Co. Ltd, Tokyo, Japan) for measurement of major inorganic nutrient concentrations [$NO_3^- + NO_2^-$, PO_4^{3-}, and $Si(OH)_4$], and (d) a 500-mL Nalgene polycarbonate bottle (Thermo Fisher Scientific Inc., Waltham, MA, USA) for measurement of chlorophyll a (chl a) concentrations. All samples were returned to the laboratory of the Japan Maritime Self-Defense Force icebreaker *Shirase* immediately after sampling. Samples for salinity and $\delta^{18}O$ analyses were stored in a refrigerator at +4°C. Samples for nutrient analyses were stored in a freezer at −30°C. Samples for chl a measurements were immediately filtered through 25-mm-diameter Whatman GF/F filters. Pigments on the filters were then extracted with *N,N*-dimethylformamide (Suzuki & Ishimaru, 1990) for more than 24 hr and stored at −30°C until analysis.

Sea ice cores were stored in a freezer at −30°C during their transport to the Institute of Low Temperature Science (ILTS), Hokkaido University, Sapporo, Japan. In the ILTS cold room (−15°C), cores were split lengthwise into two halves with an electric band saw: the first half for ice textural analysis and the second half for measurements of bulk ice salinity, $\delta^{18}O$ composition, nutrient and chl a concentrations, and cell counting for ice algae community assemblage.

2.2. Textural Analysis and the Age of an Ice Core

We examined thin ice sections to analyze ice growth processes. Ice sections 0.7 cm thick were attached to glass plates and planed down to 0.1-cm thickness with a microtome (Model SM2400, Leica Microsystems, Wetzlar, Germany). We photographed ice crystallographic structures by illuminating the thin sections placing on a light table in between the cross-polarized sheets.

Ice growth processes were examined based on our classification for sections of the ice cores as granular, columnar, or mixed ice (Eicken & Lange, 1989). Granular ice was subdivided into frazil ice and snow ice (or superimposed ice) based on its $\delta^{18}O$ value. We defined snow ice or superimposed ice as granular ice with a $\delta^{18}O$ value below that of its parent seawater (see Granskog, & Kaartokallio, 2004; Jeffries et al., 1994), taken as the $\delta^{18}O$ value of the under-ice seawater sampled during JARE60 (−0.7‰). Although coarse-grained clear ice (large, polygonal, granular crystal textures) and fine-grained opaque ice originate from superimposed and snow ice, respectively (Kawamura et al., 1997), we hereafter refer to both as "snow-origin ice" unless obviously clear ice was observed in thin section, which was described as superimposed ice. We note that the analyzed snow was thawed and moistened, and refrozen ice was observed. The snow crystal structure was an aggregate of fine particles in thin section but did not contain salt (salinity = 0); the structure sometimes became sandwiched between superimposed ice, which we refer to as "fine-grained superimposed-ice" (see details in Section 3.1).

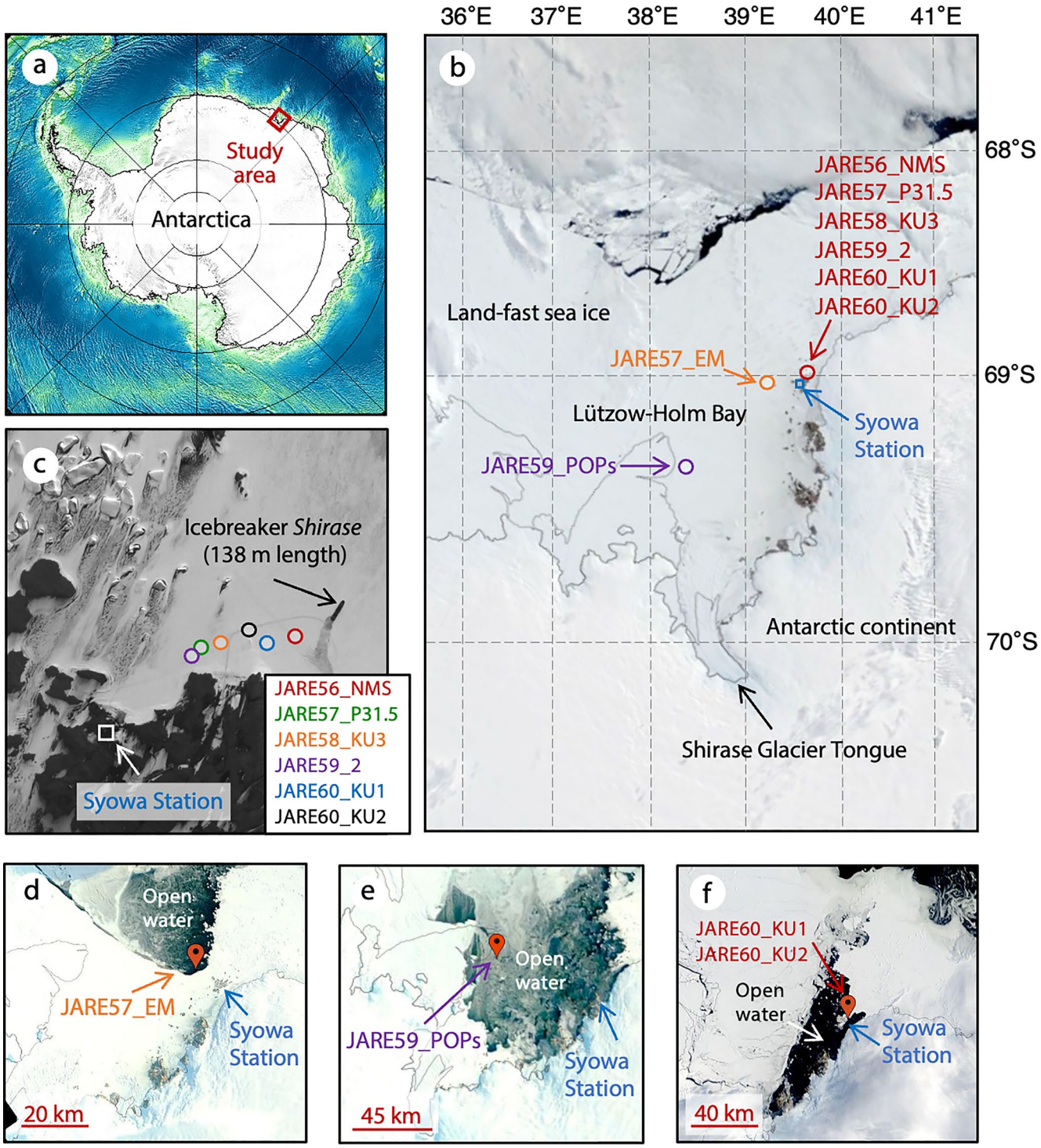

Figure 1. (a) The study area and (b)–(f) sampling locations in Lützow-Holm Bay, Eastern Antarctica. MODIS-Terra satellite images were obtained on (b) 19 January 2019, (d) 24 April 2015 at site JARE57_EM, (e) 25 April 2017 at site JARE59_POPs, and (f) 18 March 2018 at sites JARE60_KU1 and JARE60_KU2. The images in (d–f) show the sea-ice condition before winter at each coring site; dark areas indicate where the sea ice was broken, and the cores obtained from these sites were first-year ice. The background image in (c) is an Advanced Land Observing Satellite (ALOS)/Panchromatic Remote-sensing Instrument for Stereo Mapping (PRISM) image obtained on 26 January 2010 by the Japan Aerospace Exploration Agency (JAXA).

Table 1
Details of the Studied Ice Cores

Station	Position	Coring date	Ice type	Ice thickness (m)	Snow thickness (m)
JARE56 NMS	69.003°S, 39.619°E	15 January 2015	Multi-year ice	3.40	0.34
JARE57 P.31.5	69.002°S, 39.603°E	25 January 2016	Multi-year ice	4.92	0.85
JARE57 EM	69.042°S, 39.220°E	05 February 2016	First-year ice	1.32	0.05
JARE58 KU3	69.002°S, 39.606°E	05 January 2017	Multi-year ice	>2.78[a]	1.68
JARE59 2	69.002°S, 39.602°E	07 January 2018	Multi-year ice	>2.47[a]	0.78
JARE59 POPs	69.353°S, 38.326°E	27 January 2018	First-year ice	1.44	0.20
JARE60 KU1	69.003°S, 39.614°E	02 January 2019	First-year ice	1.55	0.20
JARE60 KU2	69.002°S, 39.612°E	08 January 2019	First-year ice	1.47	0.08

Note. An electromagnetic ice thickness survey near the coring sites in January 2018 revealed the ice thickness to be ~6 m. [a]Cores JARE58_KU3 and JARE59_2 sampled only the top ~3 m.

The ice type was determined according to WMO (2014) after checking satellite imagery of the sampling point, visually observing the sea ice condition at Syowa Station, and confirming the vertical profile of textural parameters (including thin section analysis) in the core. First-year ice was collected in locations where fast ice had broken up and flowed out during the previous year (Figures 1d–1f), and sea ice had reformed within the year prior to collection. According to Syowa Station records, multi-year ice has not been broken up and flowed out since March 1980 (Higashi et al., 1982; Ushio, 2006).

2.3. Sample Analysis

To measure ice salinity, water $\delta^{18}O$ composition, and nutrient and chl a concentrations, the second half of the core was trimmed into a rectangle with a cross-section of 4.5 × 2.5 cm and 12–18-cm-thick (vertical resolution) sections. To avoid contamination during sampling and handling, the outer 0.3 cm of each ice section was removed with a stainless steel plane. The ice sample was then put in a polyethylene bag (GL Science Inc., Japan) and melted in a cold room at +4°C. Snow samples were melted in the same bags and in the same cold room. Snow and sea ice melt samples were analyzed with the same protocol as for under-ice water samples, except for nutrient analyses; in snow and sea ice melt samples, nutrient samples were filtered with a 0.22-μm Durapore PVDF Membrane filter (MILLEX GV Filter unit, Merck Millipore Ltd., Germany). For ice algae community assemblage, sea ice melt water for the bottom ice section for JARE60 KU1 and 2 was subsampled into 100-mL polyethylene screw-cap vial (AS ONE Corporation, Tokyo, Japan), and an aliquot of 5-mL of Lugol's solution was added to preserve the sample.

The salinities of under-ice water and melted snow and sea-ice samples were measured with a conductivity sensor (Cond 315i, WTW GmbH, Germany). The oxygen isotopic ratio of under-ice water and melted snow and sea-ice samples were determined by mass spectrometry (DELTA plus; Finnigan MAT, San Jose, CA) via the equilibration method. The $\delta^{18}O$ value (‰) of a sample was calculated against the $^{18}O/^{16}O$ ratio of standard mean ocean water (VSMOW):

$$\delta^{18}O = \left[\frac{\left[\frac{^{18}O}{^{16}O}\right]_{Sample}}{\left[\frac{^{18}O}{^{16}O}\right]_{VSMOW}} - 1 \right] \times 1000 \quad (1)$$

The standard deviation (SD) on $\delta^{18}O$ values was 0.026‰ based on analyses of 10 subsamples of a reference water (seawater) with $\delta^{18}O = 0.241‰$. $\delta^{18}O$ value for the reference water was decided based on VSMOW. Nutrient concentrations [NO_3^-, NO_2^-, PO_4^{3-}, and $Si(OH)_4$] were measured with an auto-analyzer system (Quattro; Bran + Luebbe, Norderstedt, Germany) according to the spectrophotometric method reported by the Joint Global Ocean Flux Study (JGOFS, 1994). SDs on nutrient concentrations were 0.19, 0.002, 0.01, and 0.06 μmol L^{-1} for NO_3^-, NO_2^-, PO_4^{3-}, and $Si(OH)_4$, respectively, calculated from 15 subsamples of a standard with respective known concentrations of 23.28, 0.935, 1.55, and 56.99 μmol L^{-1}. Detection limit (3σ) on nutrient concentrations

were 0.029, 0.018, 0.025, and 0.470 μmol L^{-1} for NO_3^-, NO_2^-, PO_4^{3-}, and $Si(OH)_4$, respectively, calculated from seven blank samples. Chl a concentrations were determined by a fluorometer (Model 10AU, Turner Designs, Inc., Sunnyvale, CA). Standards (0.28–282.30 μg L^{-1} chl a) prepared from a liquid chl a standard (Wako Pure Chemical Industries Ltd., Osaka, Japan) by stepwise dilution with *N*,*N*-dimethylformamide were used to calibrate the fluorometer before analyses. The cell counting for ice algae community assemblage was examined with a microscope (Olympus, BH-T, Tokyo, Japan) 10X oculars and 40X objective.

2.4. Mass Fraction of Snow in Snow-Origin Ice

To determine the mass fraction of snow in snow-origin ice (hereafter, "snow fraction"), we used a mass balance equation (Jeffries et al., 1994, 2001):

$$f_{snow} + f_{sea} = 1 \quad (2)$$

$$f_{snow}\,\delta_{snow} + f_{sea}\,\delta_{sea} = \delta_{obs} \quad (3)$$

where f represents the mass fraction of snow or seawater, δ represents their $\delta^{18}O$ values, and the subscripts "snow," "sea," and "obs" indicate snow, under-ice seawater, and observed bulk ice, respectively. For δ_{sea}, we used the parent water $\delta^{18}O$ values collected during JARE60 rather than the value that includes the fractionation factor during seawater freezing (see Jeffries et al., 1994, 2001) because we assumed that all granular ice with a $\delta^{18}O$ value below that of the under-ice water was snow ice (Granskog et al., 2004; Jeffries et al., 1994). In addition, we assumed that granular ice with a $\delta^{18}O$ value below that of under-ice water was snow-origin ice. Based on the result obtained from the JARE60 samples, we used $\delta_{sea} = -0.7‰$. δ_{snow} was taken as the mean $\delta^{18}O$ value of snow samples (−20.3‰) collected during JARE56–60. We estimated the errors on the snow fractions to be less than 12.2% by calculating the effect of changing the snow $\delta^{18}O$ values by their standard deviation (±2.1‰).

3. Results and Discussion

3.1. Vertical Profiles of Sea-Ice Salinity, $\delta^{18}O$ Values, and Sea-Ice Structure

Over the study period, first-year ice and snow on ice were ranged between 1.32 and 1.55 m thick and 0.05 and 0.20 m deep, respectively (Table 1). Multi-year ice and snow on ice ranged between >2.47 and ca. 6 m thick and 0.34 and 1.68 m deep, respectively (Table 1). Figure 2 shows vertical salinity and $\delta^{18}O$ profiles for both first-year and multi-year ice cores. The salinity of the first-year ice was close to 0 near the ice–snow interface and increased with increasing depth until reaching a maximum, after which it decreased with increasing depth (Figure 2a). Salinity again increased at the bottom of some cores, giving the salinity profiles of first-year ice a characteristic "C" shape (excluding the topmost low-salinity ice). $\delta^{18}O$ values in first-year ice were as low as −20‰ near the ice–snow interface (Figure 2b) and increased with increasing depth, reaching values above that of the under-ice water (−0.7‰) by the middle of the core. The profiles record low salinity and $\delta^{18}O$ values near the ice–snow interface because the cores were collected in late summer (Table 1), by which time the accumulated snow had become snow-origin ice due to melting of the sea-ice surface in above-freezing air temperatures and strong sunlight (Nomura, Simizu, et al., 2011). Furthermore, in late summer, the nighttime air temperature becomes negative in this area (Nomura, Simizu, et al., 2011), freezing any water that had melted during the day. Because the snow depths were quite small relative to the ice thickness (Table 1) and the salinity was extremely low, especially near the ice surface, we considered that the ice formed was superimposed ice rather than snow ice because snow ice should only form when the snow depth is large with respect to the ice thickness (Maksym & Jeffries, 2000; Sturm & Massom, 2017). Indeed, in thin section, we observed large, polygonal, granular crystal textures (photograph in Figure 2a) characteristic of superimposed ice (Kawamura et al., 2004) near the ice surface.

The bulk ice salinity of multi-year ice was 0 from the ice–snow interface to depths of around −100 cm (Figure 2c), then generally increased with increasing depth. The maximum observed salinity was 3.8 in core JARE58_KU3. At the bottom of the ice column, salinities were about 1–3. The $\delta^{18}O$ values of sea ice were similar to those of the overlying snow from the ice–snow interface to depths of −200 cm (Figure 2d), then increased with increasing depth. The ice $\delta^{18}O$ values reached that of the under-ice water at depths of −300 cm in core JARE56_NMS and −380 cm in core JARE57_P31.5. These results indicate that snow cover affects to a maximum depth of −380 cm.

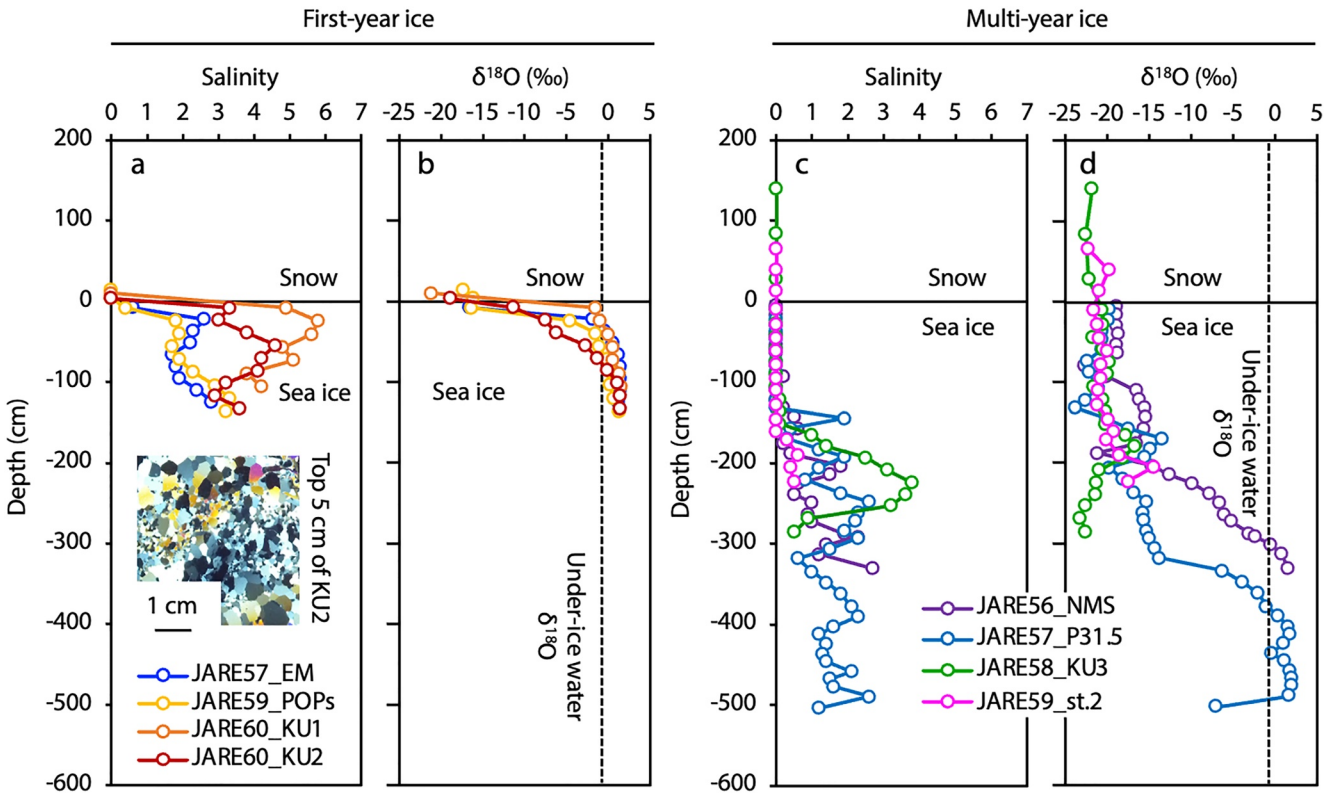

Figure 2. Vertical profiles of (a), (c) salinity and (b), (d) $\delta^{18}O$ values in snow, first-year ice cores (left), and multi-year ice cores (right). Horizontal solid lines at 0 cm depth indicate the snow–ice interface. Dashed lines in (b), (d) show the $\delta^{18}O$ value of under-ice water (−0.7‰) sampled during JARE60. The photo in (a) is a vertical thin section of the top 5 cm of core JARE60_KU2.

Comparisons of the salinity and $\delta^{18}O$ profiles of multi-year ice core JARE57_P31.5 to the interpreted ice structure and photographs of representative thin sections were shown in Figure 3. Up to a depth of −117 cm, salinity and $\delta^{18}O$ were maintained at 0 and −20‰, respectively (Figure 3a). Because most of this upper section of the core comprised coarse-grained (large polygonal) granular ice, we concluded that it was superimposed ice (Figures 3b and 3c; Kawamura et al., 2004). In addition, fine-grained granular ice was present at depths from −100 to −117 cm (Figures 3b and 3d). Based on the salinity and textures down to a depth of −117 cm, it is unlikely that snow ice was formed by the infiltration of seawater. In addition, the small crystal size at depths of −100 to −117 cm (Figure 3d) indicated that this ice corresponded to superimposed ice formed from wet, unmelted snow that had re-frozen at negative temperatures, which we refer to as fine-grained superimposed ice.

At depths of −117 to −170 cm, sea ice salinity and $\delta^{18}O$ values increased (Figure 3a) and the ice structure became columnar (Figures 3b and 3e), with larger grains than in the overlying fine-grained granular ice. However, the columns were neither as wide nor as vertically extended as those of columnar ice formed from seawater (Figure 3f, see next paragraph). Based on the salinity and $\delta^{18}O$ values of the ice, this structural transformation occurred because the ice formed from snowmelt water with a slight seawater influence. Therefore, we suspect that this ice formed from a refrozen mixture of seawater and snowmelt. Indeed, in this area, it has been reported that a layer of superimposed ice forms under the snow, and that a slush layer (puddles in the sea ice that are likely snowmelt ponds) forms under the superimposed ice (Nomura et al., 2018). In that study, the salinity and $\delta^{18}O$ values of the slush layer were ≤1 and −20‰, respectively, because snowmelt was supplied mainly from above (as snow or superimposed ice), and a small amount of seawater was transported upwards through a crack and then horizontally transported into the slush layer. The salinity and $\delta^{18}O$ values of their slush layer were approximately the same as those of the columnar ice measured in our study (Figure 3a). The slush layer is about 10–20 cm thick (Nomura et al., 2012) and, in winter, is thought to freeze from the top faster than columnar ice develops at greater depths in the sea ice. Therefore, we consider that the columns in this zone are thinner and shorter than those in columnar ice formed from seawater (Figures 3e and 3f) because the freezing speed affects the crystal structure, hexagonal ice

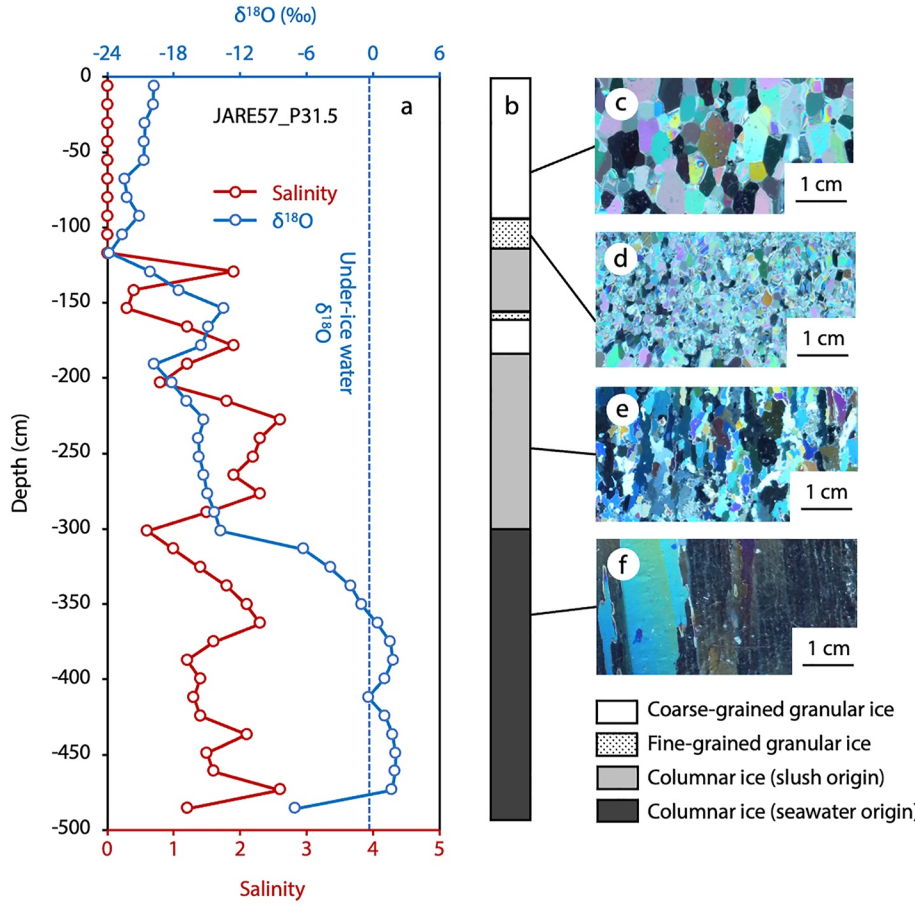

Figure 3. (a) Vertical profiles of salinity and $\delta^{18}O$ values in core JARE57_P31.5 compared to (b) its ice structure. (c)–(f) Representative vertical thin section photographs are provided for each ice structure.

(Ih) with three a-axes lying in the basal plane and a c-axis pointing perpendicular to this plane (Pauling, 1935), with slower growth on the c-axis direction than the basal plane (e.g., Hillig, 1959). Both fine- and coarse-grained granular ice have random crystal texture (Figures 3c and 3d). As the freezing develops, geometric selection sweep away crystals with c-axis perpendicular to the ice–ocean interface (Kolmogorov, 1976). The crystals in the slush layer that have the c-axes pointing radially (perpendicular to the ice–ocean interface) grow faster than those with c-axes pointing parallel to the ice–ocean interface. Therefore, it seems likely that the columns in slush layer was thinner due to the initial stage of geometric selection and shorter than those in columnar ice formed from seawater constrained by the slush layer thickness. In this study, we refer to this particular columnar ice texture as "slush-origin columnar ice," in contrast to columnar ice formed from seawater ("seawater-origin columnar ice").

A distinct unit comprising a fine-grained granular ice layer overlying a coarse-grained granular ice layer was sandwiched between slush-origin columnar ices at depths of −170 to −190 cm. This unit formed because superimposed ice formed under the snow (Nomura et al., 2018) and a slush layer below it. This is thought to reflect greater amounts of snowfall in following years, with the slush layer being repeatedly formed and refrozen. The underlying slush-origin columnar ice layer extended to a depth of −300 cm, where the ice structure became columnar, but of seawater origin.

In contrast, the first-year ice was predominantly columnar (Table 2). From the above discussion, snow accumulates on the ice year-by-year, causing flooding and slush formation, then refreezing in winter. Furthermore, when the ice thickness increases, flooding ceases, and the snowmelt is refrozen. This upward growth is characteristic of Antarctic multi-year ice (Kawamura et al., 1997; Nomura et al., 2018), although the collection of a nearly 5-m sea-ice core has never been reported. This is thus the first time that the characteristics of the upward growth of multi-year fast ice have been shown based on multiple years of repeated ice coring.

Table 2
The Disctribution of Ice Structures Over the Total Length of Each Ice Core

Sampling station	Ice type	Fraction (%)		
		Coarse granular	Fine granular	Columnar
JARE56_NMS	Multi-year ice	–[a]	–[a]	–[a]
JARE57_P31.5	Multi-year ice	22.4	0.6	71.5
JARE57_EM	First-year ice	5.6	5.6	88.9
JARE58_KU3[b]	Multi-year ice	83.1	7.6	9.4
JARE59_2[b]	Multi-year ice	74.1	4.5	21.5
JARE59_POPs	First-year ice	0.0	2.1	97.9
JARE60_KU1	First-year ice	0.0	43.2	56.8
JARE60_KU2	First-year ice	3.4	17.7	78.9

[a]No data. [b]Data represent only the top ~3 m of the core (see Table 1).

3.2. Vertical Profiles of Sea-Ice Nutrient Concentrations

Vertical profiles of NO_3^-, PO_4^{3-}, and $Si(OH)_4$ concentrations in first-year and multi-year ice were shown in Figure 4. NO_3^- concentrations in first-year ice varied widely with depth in core JARE60_KU1 (0–2.6 μmol L^{-1}), but were in the range 0–1 μmol L^{-1} in other cores (Figure 4a). NO_3^- concentrations in multi-year ice were 0–0.5 μmol L^{-1} in the top half of the ice column, and the first maximum at those depths, peaking at ~1.0 μmol L^{-1}, was observed at a depth of −200 cm in some ice cores (Figure 4e). At greater depths in the cores, NO_3^- concentrations were as low as 0–0.5 μmol L^{-1}, and the maximum of 3.5 μmol L^{-1} was observed at the bottom of the sea ice. In first-year ice, PO_4^{3-} concentrations varied between cores but were fairly constant at shallow to medial depths, and were greatest at the bottom of the ice column (Figure 4b). In multi-year ice, however, PO_4^{3-} concentrations were extremely low from the ice–snow interface to a depth of −150 cm, and the maximum concentration of 1.6 μmol L^{-1} was observed at a depth of −360 cm in core JARE57_P31.5 (Figure 4f). $Si(OH)_4$ concentrations varied little with depth in the first-year ice (Figure 4c), but mimicked the PO_4^{3-} profile in multi-year ice.

Our results show clear differences between the vertical nutrient profiles in first-year and multi-year ice (Figure 4). First-year ice generally has the lowest nutrient concentrations in snow, and concentrations increase slightly in sea ice, but they remain relatively constant until peaking at the bottom of the ice column (Figures 4a–4c). In contrast, in multi-year ice, the upper half of the ice column was nutrient poor, similar to the overlying snow, and nutrient concentrations increased from the middle of the column to maximum concentrations in the bottom half of the column (Figures 4e–4g). Because nutrient concentrations in snow were consistently low (Figures 4e–4g), the upper half of the multi-year ice columns, comprising snow-origin ice, also contained low nutrient concentrations.

Such vertical nutrient distributions are considered to be closely related to physical characteristics such as salinity, $\delta^{18}O$ value, and ice structure (discussed in Section 3.3). Furthermore, the high concentrations of various nutrients at the bottom of both first-year and multi-year ice columns are most likely related to the high concentrations of chl a in the bottommost ice column (Figures 4d and 4h), indicating both photosynthesis by the ice algae and remineralization by the degradation of organic matter (Roukaerts et al., 2021; Rysgaard & Glud, 2004; Rysgaard et al., 2008; Thomas et al., 1995). Roukaerts et al. (2021) proposed the microbial biofilm in sea ice. In the microbial biofilm, accumulation in the macro-nutrients (high nutrients) coincides with an accumulation of autotrophic biomass (high chl a).

The mean value and standard deviation of each nutrient component and physical parameter are reported in Table 3 for snow and each sea-ice type. Nutrient and chl a concentrations were low in snow and superimposed ice and particularly high in columnar ice. In contrast, snow-ice, which is affected by both snow and seawater, had intermediate nutrient and chl a concentrations. Our results clearly indicate that a greater snow influence results in lower nutrient and chl a concentrations in sea ice.

3.3. Variations of Nutrient Concentrations in Snow-Origin Ice

In Section 3.2, we showed that in multi-year ice columns, nutrient concentrations were lower in snow-origin ice than in columnar ice (Table 3). To quantify the effect of snow on sea-ice nutrient concentrations, we calculated the snow fraction in snow-origin ice (Equations 1 and 2) to examine the relationship between nutrient concentrations and snow fraction (Figure 5). Although the regressions differed between nutrients, nutrient concentrations tended to decrease with increasing snow fraction. This is due to the purity of the air near Antarctica, being far from areas of human activity, compared to that in the Northern Hemisphere. Therefore, the atmospheric transfer and deposition of nutrients onto sea ice is limited in Antarctica, and the top surface of the sea ice is replaced by clean, snow-origin ice. In contrast, in the Northern Hemisphere, atmospheric transfer and deposition of polluted snow is known to be a potential source of nutrients for sea ice (Granskog & Kaartokallio, 2004; Granskog et al., 2003; Kaartokallio, 2001; Krell et al., 2003; Nomura et al., 2010; Nomura, McMinn, et al., 2011b; Rahm et al., 1995). Although nutrient concentrations for snow-origin ice were generally decreased as the snow fraction

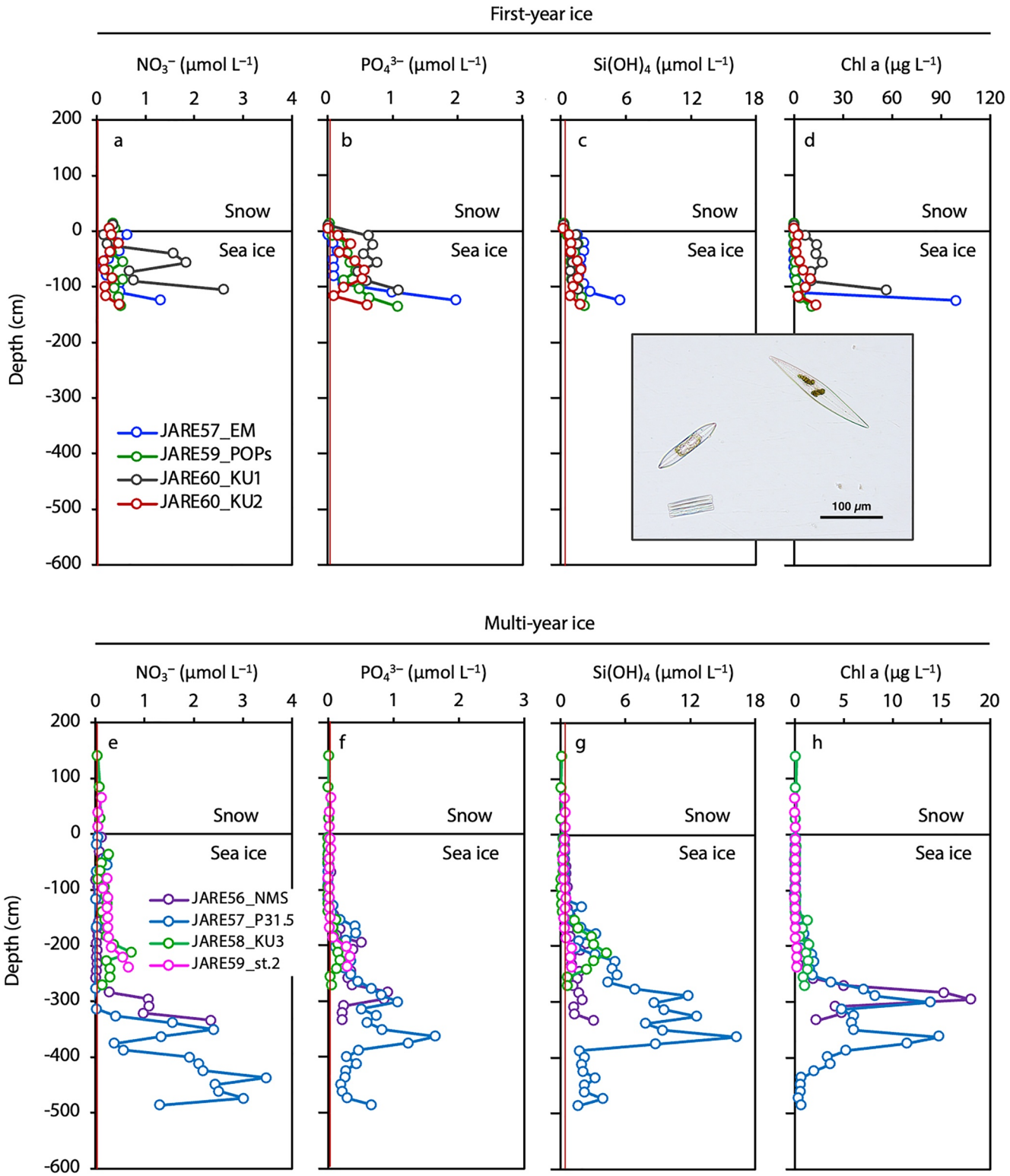

Figure 4. Vertical profiles of (a), (e) NO_3^-, (b), (f) PO_4^{3-}, (c), (g) $Si(OH)_4$, and (d), (h) chl a concentrations in first-year ice (top) and multi-year ice cores (bottom). Horizontal solid lines at a depth of 0 cm indicate the snow–ice interface. The photo in (c) and (d) is the ice algae community assemblage for the bottom of core JARE60_KU1. Red lines for nutrient vertical profiles indicate the detection limit for nutrients concentration.

Table 3
Salinity, $\delta^{18}O$ Values, and Nutrient and Chl a Concentrations (Mean ± Standard Deviation) in Snow and Each Ice Type

Snow and ice type	Salinity (–)	$\delta^{18}O$ (‰)	PO_4^{3-}– (μmol L^{-1})	$Si(OH)_4$ (μmol L^{-1})	NO_3– (μmol L^{-1})	NO_2– (μmol L^{-1})	Chl a (μg L^{-1})
Snow ($n = 10$)	0.0 ± 0.0	−20.3 ± 2.1	0.0 ± 0.0	0.0 ± 0.2	0.2 ± 0.1	0.00 ± 0.01	0.1 ± 0.1
Superimposed ice ($n = 27$)	0.0 ± 0.0	−20.9 ± 1.0	0.0 ± 0.0	0.0 ± 0.1	0.1 ± 0.2	0.00 ± 0.01	0.0 ± 0.0
Snow ice ($n = 24$)	2.2 ± 1.8	−15.2 ± 7.5	0.2 ± 0.2	1.1 ± 1.1	0.4 ± 0.4	0.01 ± 0.02	2.9 ± 4.9
Columner ice ($n = 16$)	2.2 ± 1.1	−4.6 ± 7.6	0.5 ± 0.4	3.0 ± 3.4	0.7 ± 0.9	0.03 ± 0.02	6.4 ± 14.9

increased (Figure 5), NO_3^- and $Si(OH)_4$ concentrations notably differed, with no correlation between snow fraction (Figures 5b and 5c).

Due to the formation of snow-origin ice, the snow fraction in multi-year ice increased year-by-year; the mean snow fractions in the top 200 cm of multi-year ice gradually increased from about 88% in 2015% to 100% by 2018 (Figure 6). Therefore, our sea-ice core samples record a steady increase in the contribution of snow to sea ice. Although we have not collected multi-year ice cores at distant locations within the same year (Figure 1c) and thus have not been able to unequivocally determine that there is no spatial bias in our sampling, the nutrient concentrations do not differ greatly between sampling locations, and the trends and profiles are similar from year to year (Figures 2 and 4).

3.4. Variations of Nutrient Concentrations in Seawater-Origin Ice

Although nutrient concentrations decreased as the snow fraction increased in the top layer of sea ice, the distributions of nutrient concentrations differed among the different nutrient components (Figure 5). Therefore, we here evaluate the effects of primary production, and organic matter remineralization on nutrient concentrations in both first-year and multi-year ice. We compared salinity to nutrient concentrations (Figure 7). Sea-ice salinity is a conservative component that only changes through physical processes such as brine drainage or exchange with under-ice water. Therefore, we investigated deviations from a dilution line based on the salinity and nutrient concentrations of the under-ice water collected during JARE60 to understand the biological processes affecting the nutrient distributions in the sea ice. Data plotted above the dilution line indicates nutrient supply due to the

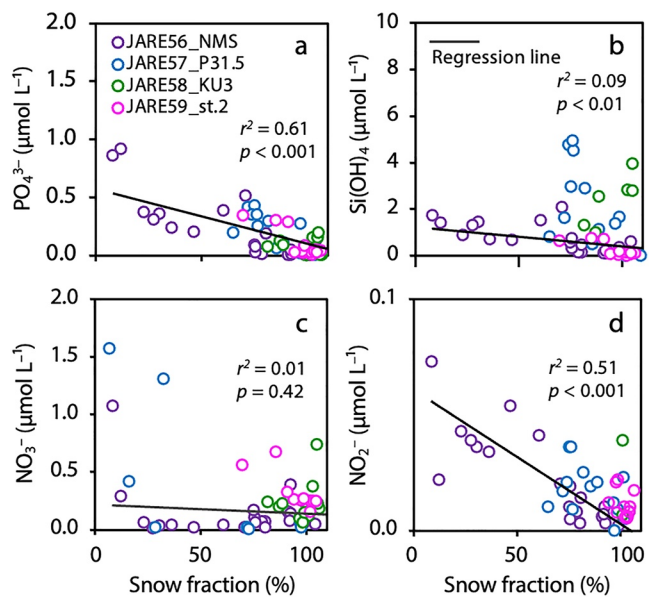

Figure 5. Plots of (a) PO_4^{3-}, (b) $Si(OH)_4$, (c) NO_3^-, and (d) NO_2^- concentrations for snow-origin ice versus snow fraction in multi-year ice cores.

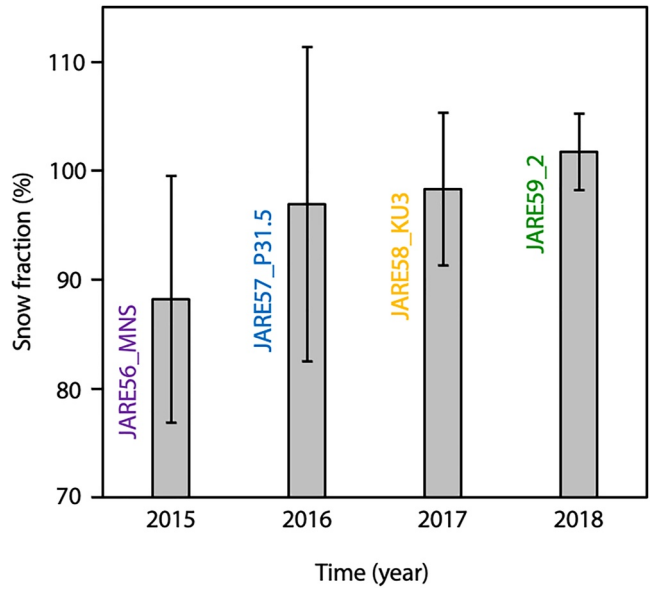

Figure 6. Time series of the mean snow fraction in the top 200 cm of each multi-year ice core from 2015 (core JARE56_NMS) to 2018 (core JARE59_2).

remineralization of organic matter by heterotrophic organisms and bacteria in the sea ice or from external sources (e.g., the atmosphere); conversely, data points below the dilution line indicate nutrient uptake by ice algae during primary production (e.g., Thomas et al., 1995). We tried to take under-ice water samples through the ice core hole for every station. However, it was difficult to pass though the ice core hole until the bottom of the thick ice due to thick ice (about 5 m). In addition, even if we pass through the ice core hole, the under-ice water sampling was difficult due to narrow (10 cm diameter) and long (5 m thick ice) hole. Therefore, we could not get under-ice water for every station. We compared our data with the ship-based data obtained in the Lützow-Holm Bay near Syowa Station (Kiuchi et al., 2021). In Kiuchi et al. (2021), salinity was 34.0 at 20 m depth (shallowest depth) in Station D6 (closest station from Syowa Station) on 31 January 2017. We also checked other stations (D5, E5, and E6: closest station for D6), and the range of salinity was between 34.0 and 34.1 (see Table S1). These results indicated that the salinity used in our study (33.9) was same as the salinity in the Lützow-Holm Bay near Syowa Station (Kiuchi et al., 2021). Therefore, we believe that it is reasonable to use the salinity (33.9) as dilution lines.

$Si(OH)_4$ concentrations in first-year ice locate significantly below the dilution line (Figure 7a), whereas those in multi-year ice are closer to or above the dilution line (Figure 7b). The distributions of chl a concentrations in the sea ice (Figures 4d and 4h) indicate the presence of ice algae, which would mainly be diatoms (*Fragilariopsis* sp. and *Pleurosigma* sp. (photo in Figures 4c and 4d) based on the cell counting for ice algae community assemblage in this study. Indeed, in first-year ice, primary production by diatoms consumes a large amount of $Si(OH)_4$ (Tréguer & De La Rocha, 2013), and the slow dissolution of diatom frustules should limit the resupply of $Si(OH)_4$. In contrast, in multi-year ice, the more protracted dissolution of diatom frustules should resupply $Si(OH)_4$, eventually balancing the consumption of $Si(OH)_4$ by primary production. However, in core JARE57_P31.5 (the deepest core studied), $Si(OH)_4$ concentrations plot well above the dilution line (Figure 7b), indicating that the resupply of $Si(OH)_4$ by dissolution of diatom frustules exceeded consumption.

Consistent with a previous sampling at the same location (Nomura et al., 2018), PO_4^{3-} concentrations plot above the dilution line in both first-year and multi-year ice (Figures 7c and 7d), suggesting resupply by the remineralization of organic matter. The difference in the resupply rates of PO_4^{3-} and $Si(OH)_4$ is due to the fact that the remineralization of PO_4^{3-} is faster than the dissolution of $Si(OH)_4$ (Fripiat et al., 2017). Arrigo et al. (1995) calculated the high remineralization rates (35 μmol L^{-1} d^{-1}) for PO_4^{3-} for the platelet-ice communities of McMurdo Sound, Antarctica. Such high remineralization rates were considered due to bacteria or protozoan metabolism (Grossmann et al., 1996; Thomas & Dieckmann, 2002).

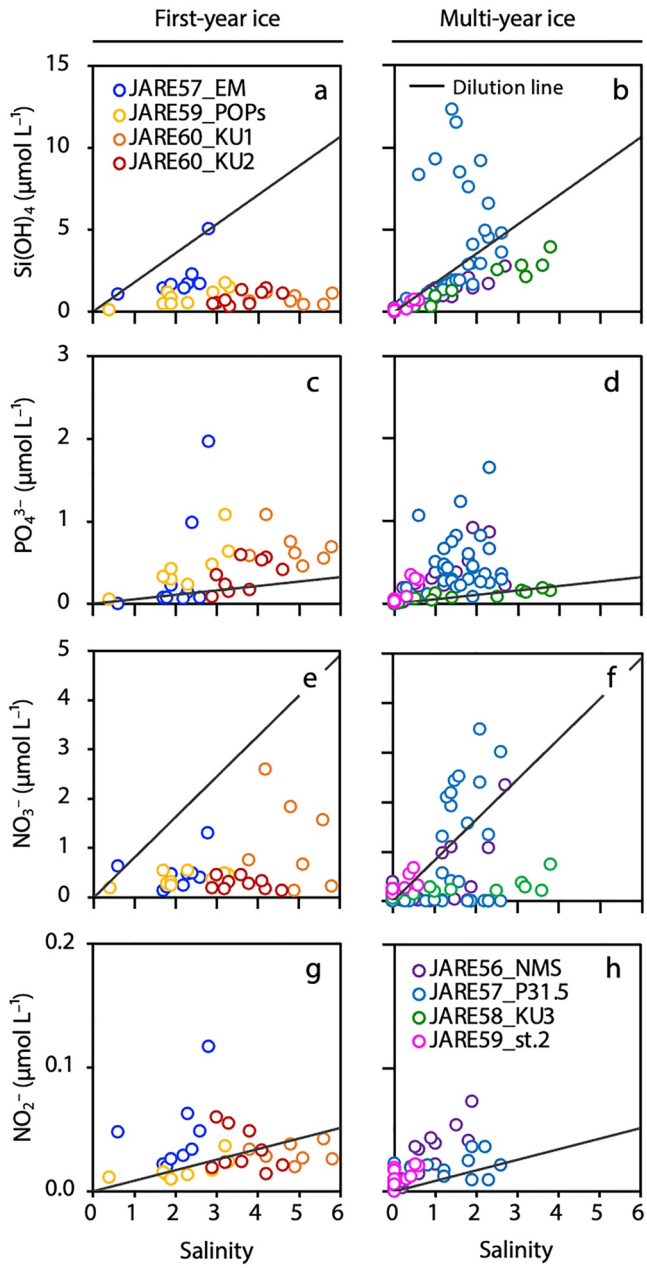

Figure 7. Plots of (a), (b) $Si(OH)_4$, (c), (d) PO_4^{3-}, (e), (f) NO_3^-, and (g), (h) NO_2^- concentrations versus salinity in first-year (left) and multi-year ice cores (right). Dilution lines are based on the nutrient concentrations and salinity of under-ice water.

NO_3^- concentrations in most first-year and multi-year ice cores plot below the dilution line (Figures 7e and 7f). This is expected for first-year ice, in which primary production consumes NO_3^-, as with $Si(OH)_4$ and PO_4^{3-}. The PO_4^{3-} concentrations are even higher than the NO_3^- concentrations with respect to the dilution line (Figures 7c–7f), likely indicating that remineralization of particulate organic phosphate to PO_4^{3-} proceeds more rapidly than the remineralization of particulate organic nitrogen to NH_4^+ and nitrification of NH_4^+ to NO_3^- (Fripiat et al., 2017). Grosmann et al. (1996) observed that PO_4^{3-} in the platelet-ice clearly exceeded that in the water column while NO_3^- concentrations were low in the platelet-ice than those in water column in the Weddell Sea during late austral summer. These results support the higher remineralization rate of PO_4^{3-} than that of NO_3^-.

4. Conclusions

We investigated the effects of snow cover on the vertical distribution of nutrient concentrations and the long-term remineralization process in multi-year, Antarctic fast sea ice. We analyzed thin sections to determine the ice structure, which confirmed the upward growth of fast ice by the year-by-year formation of snow-origin ice. Vertical profiles of biogeochemical components in the ice showed that the high nutrient concentrations of first-year ice are transported downward by the subsequent formation of new snow-origin ice, eventually forming multi-year ice. Because the atmospheric nutrient supply is limited by the purity of Antarctic snow, nutrient concentrations in snow-origin ice decreased as the snow fraction increased.

Nutrients incorporated into columnar ice of seawater origin were dominantly processed by biological uptake via primary production during the first year, but remineralization of degrading organic matter by heterotrophic organisms and bacteria resupplied nutrients to multi-year ice. By analyzing data on first-year and multi-year ice spanning several years in the same area, it was possible for the first time to determine the long-term cycling of nutrients in fast ice.

Data Availability Statement

The data used in this study are available in the supplementary information (Table S1) and are archived in the data repository of the National Institute of Polar Research, Tokyo, Japan (https://ads.nipr.ac.jp/data/meta/A20220705-001).

Acknowledgments
We express our heartfelt thanks to the sea ice team, members of the JARE, the crew of the Japan Maritime Self-Defense Force icebreaker *Shirase*, and cruise members for their support in conducting field work. We thank Prof. K. Kawashima, K. Murakami, H. Nakajima, M. Kiuchi, T. Ishino, and T. P. Tamura for their support in the low temperature room, M. Hirabayashi for oxygen isotopic analyses, and A. Ooki for nutrient analyses. We benefitted greatly from advice and useful comments on the nutrient data offered by A. Ooki and T. Ishino. This work was supported by grants from the Japan Society for the Promotion of Science (Nos. 17H04715, 17H04710, 17H06317, 17H06322, 18F18794, 20H04345, 21H04931), the Science Program of the Japanese Antarctic Research Expedition (JARE) as Prioritized Research AJ0902 (ROBOTICA), the National Institute of Polar Research (NIPR) through Project Research KP-303 and General Collaboration Project Nos. 28–14, 2–13 and the grant for young scientist, the Center for the Promotion of Integrated Sciences of SOKENDAI, and the Joint Research Program of the Institute of Low Temperature Science, Hokkaido University.

References

Ackley, S. F., & Sullivan, C. W. (1994). Physical controls on the development and characteristics of Antarctic sea ice biological communities— A review and synthesis. *Deep Sea Research Part I: Oceanographic Research Papers*, *41*, 1583–1604. https://doi.org/10.1016/0967-0637(94)90062-0

Aoki, S. (2017). Breakup of land-fast sea ice in Lützow-Holm Bay, East Antarctica, and its teleconnection to tropical Pacific sea surface temperatures. *Geophysical Research Letters*, *44*, 3219–3227. https://doi.org/10.1002/2017gl072835

Arrigo, K. R. (2017). Sea ice as a habitat for primary producers. In D. N. Thomas (Ed.), *Sea ice* (3rd ed., pp. 352–369). Chichester, UK: Wiley-Blackwell. https://doi.org/10.1002/9781118778371.ch14

Arrigo, K. R., Dieckmann, G. S., Gosselin, M., Robinson, D. H., Fritsen, C. H., & Sullivan, C. W. (1995). High resolution study of the platelet ice ecosystem in McMurdo Sound, Antarctica: Biomass, nutrient, and production profiles within a dense microalgal bloom. *Marine Ecology Progress Series*, *127*, 255–268. https://doi.org/10.3354/meps127255

Arrigo, K. R., Mock, T., & Lizotte, M. P. (2010). Primary producers and sea ice. In D. N. Thomas, & G. S. Dieckmann (Eds.), *Sea ice* (2nd ed., pp. 283–325). Wiley-Blackwell. https://doi.org/10.1002/9781444317145.ch8

Eicken, H., & Lange, M. (1989). Development and properties of sea ice in the coastal regime of the southern Weddell Sea. *Journal of Geophysical Research*, *94*, 8193–8206. https://doi.org/10.1029/JC094iC06p08193

Fraser, A. D., Massom, R. A., Handcock, M., Reid, P., Ohshima, K. I., Raphael, M., et al. (2021). Eighteen-year record of circum-Antarctic landfast-sea-ice distribution allows detailed baseline characterisation and reveals trends and variability. *The Cryosphere*, *15*(11), 5061–5077. https://doi.org/10.5194/tc-15-5061-2021

Fraser, A. D., Massom, R. A., Michael, K. J., Galton-Fenzi, B. K., & Lieser, J. L. (2012). East Antarctic landfast sea ice distribution and variability, 2000–08. *Journal of Climate*, *25*, 1137–1156. https://doi.org/10.1175/JCLI-D-10-05032.1

Fripiat, F., Meiners, K. M., Vancoppenolle, M., Papadimitrio, S., Thomas, D. N., Ackley, S. F., et al. (2017). Macro-nutrient concentrations in Antarctic pack ice: Overall patterns and overlooked processes. *Elementa Science of Anthropocene*, *5*, 13. https://doi.org/10.1525/elementa.217

Fritsen, C. H., Lytle, V. I., Ackley, S. F., & Sullivan, C. W. (1994). Autumn bloom of Antarctic pack-ice algae. *Science*, *266*, 782–784. https://doi.org/10.1126/science.266.5186.782

Gleitz, M., Vonderlo, M. R., Tomas, D. N., Dieckmann, G. S., & Millero, F. J. (1995). Comparison of summer and winter inorganic carbon, oxygen and nutrient concentrations in Antarctic sea ice brine. *Marine Chemistry*, *51*, 81–89. https://doi.org/10.1016/0304-4203(95)00053-T

Granskog, M. A., & Kaartokallio, H. (2004). An estimation of the potential fluxes of nitrogen, phosphorus, cadmium and lead from sea ice and snow in the northern Baltic Sea. *Water Air Soil Pollution*, *154*, 331–347. https://doi.org/10.1023/b:wate.0000022975.74321.27

Granskog, M. A., Kaartokallio, H., & Shirasawa, K. (2003). Nutrient status of Baltic sea ice: Evidence for control by snow–ice formation, ice permeability, and ice algae. *Journal of Geophysical Research: Oceans*, *108*(C8), 3253. https://doi.org/10.1029/2002JC001386

Granskog, M. A., Leppäranta, M., Kawamura, T., Ehn, J., & Shirasawa, K. (2004). Seasonal development of the properties and composition of landfast sea ice in the Gulf of Finland, the Baltic Sea. *Journal of Geophysical Research: Oceans*, *109*(C2), C02020. https://doi.org/10.1029/2003jc001874

Grossmann, S., Lochte, K., & Scharek, R. (1996). Algal and bacterial processes in platelet ice during late austral summer. *Polar Biology*, *16*, 623–633. https://doi.org/10.1007/BF02329060

Higashi, A., Goodman, D. J., Kawaguchi, S., & Mae, S. (1982). The cause of the breakup of fast ice on March 18, 1980 near Syowa station, East Antarctica. *Memoirs of National Institute of Polar Research*, *24*, 222–231.

Hillig, W. (1959). Kinetics of solidification from nonmetallic liquids. In W. Kingery (Ed.), *Kinetics of high-temperature processes* (pp. 127–135). MIT Press.

Jeffries, M., Shaw, R., Morris, K., Veazey, A., & Krouse, H. (1994). Crystal structure, stable isotopes ($\delta^{18}O$), and development of sea ice in the Ross, Amundsen, and Bellingshausen seas, Antarctica. *Journal of Geophysical Research: Oceans*, *99*(C1), 985–995. https://doi.org/10.1029/93JC02057

Jeffries, M. O., Krouse, H. R., Hurst-Cushing, B., & Maksym, T. (2001). Snow-ice accretion and snow-cover depletion on Antarctic first-year sea-ice floes. *Annals of Glaciology*, *33*, 51–60. https://doi.org/10.3189/172756401781818266

JGOFS. (1994). *Protocols for the Joint Global Ocean flux study core measurements*. *International JGOFS Report Series* (Vol. 19). JGOFS International Project Office.

Kaartokallio, H. (2001). Evidence for active microbial nitrogen transformations in sea ice (Gulf of Bothnia, Baltic Sea) in midwinter. *Polar Biology*, *24*, 21–28. https://doi.org/10.1007/s003000000169

Kattner, G., Thomas, D. N., Haas, C., Kennedy, H., & Dieckmann, G. S. (2004). Surface ice and gap layers in Antarctic sea ice: Highly productive habitats. *Marine Ecology Progress Series*, *277*, 1–12. https://doi.org/10.3354/meps277001

Kawamura, T., Jeffries, M., Tison, J., & Krouse, H. (2004). Superimposed-ice formation in summer on Ross Sea pack-ice floes. *Annals of Glaciology*, *39*, 563–568. https://doi.org/10.3189/172756404781814168

Kawamura, T., Ohshima, K. I., Takizawa, T., & Ushio, S. (1997). Physical, structural, and isotopic characteristics and growth processes of fast sea ice in Lützow-Holm Bay-Holm Bay, Antarctica. *Journal of Geophysical Research: Oceans*, *102*, 3345–3355. https://doi.org/10.1029/96jc03206

Kiuchi, M., Nomura, D., Hirano, D., Tamura, T., Hashida, G., Ushio, S., et al. (2021). The effect of basal melting of the Shirase Glacier Tongue on the CO_2 system in Lützow-Holm Bay, East Antarctica. *Journal of Geophysical Research-Biogeosciences*, *126*, e2020JG005762. https://doi.org/10.1029/2020JG005762

Kolmogorov, A. N. (1976). *Geometric selection of crystals*. Doklady Akad Nauk Minerologia USSR, (Vol. 65(5), pp. 681–684).

Krell, A., Ummenhofer, C., Kattner, G., Naumov, A., Evans, D., Dieckmann, G. S., et al. (2003). The biology and chemistry of land fast ice in the white sea, Russia—A comparison of winter and spring conditions. *Polar Biology*, *26*, 707–719. https://doi.org/10.1007/s00300-003-0543-7

Lim, S. M., Moreau, S., Vancoppenolle, M., Deman, F., Roukaerts, A., Meiners, K. M., et al. (2019). Field observations and physical-biogeochemical modeling suggest low silicon affinity for Antarctic fast-ice diatoms. *Journal of Geophysical Research: Oceans*, *124*(11), 7837–7853. https://doi.org/10.1029/2018jc014458

Maksym, T., & Jeffries, M. O. (2000). A one-dimensional percolation model of flooding and snow-ice formation on Antarctic sea ice. *Journal of Geophysical Research*, *105*(C11), 26313–26331. https://doi.org/10.1029/2000JC900130

Nomura, D., Aoki, S., Simizu, D., & Iida, T. (2018). Influence of sea ice crack formation on the spatial distribution of nutrients and microalgae in flooded Antarctic multiyear ice. *Journal of Geophysical Research: Oceans*, *123*, 939–951. https://doi.org/10.1002/2017JC012941

Nomura, D., Koga, S., Kasamatsu, N., Shinagawa, H., Simizu, D., Wada, M., et al. (2012). Direct measurements of DMS flux from Antarctic fast sea ice to the atmosphere by a chamber technique. *Journal of Geophysical Research-Oceans*, *117*, C04011. https://doi.org/10.1029/2010JC006755

Nomura, D., McMinn, A., Hattori, H., Aoki, S., & Fukuchi, M. (2011). Incorporation of nitrogen compounds into sea ice from atmospheric deposition. *Marine Chemistry*, *127*, 90–99. https://doi.org/10.1016/j.marchem.2011.08.002

Nomura, D., Nishioka, J., Granskog, M. A., Krell, A., Matoba, S., Toyota, T., et al. (2010). Nutrient distributions associated with snow and sediment-laden layers in sea ice of the southern Sea of Okhotsk. *Marine Chemistry*, *119*, 1–4. https://doi.org/10.1016/j.marchem.2009.11.005

Nomura, D., Simizu, D., Shinagawa, H., Oouchida, C., & Fukuchi, M. (2011). Biogeochemical properties of water in surface ponds on Antarctic fast ice and relationship to underlying sea ice properties. *Journal of Glaciology*, *57*, 205. 1–9. https://doi.org/10.3189/002214311798043825

Nomura, D., Takatsuka, T., Ishikawa, M., Kawamura, T., Shirasawa, K., & Yoshikawa-Inoue, H. (2009). Transport of chemical components in sea ice and under-ice water during melting in the seasonally ice-covered Saroma-ko Lagoon, Hokkaido, Japan. *Estuarine, Coastal and Shelf Science*, *81*, 201–209. https://doi.org/10.1016/j.ecss.2008.10.012

Pauling, L. (1935). The structure and entropy of ice and of other crystals with some randomness of atomic arrangement. *Journal of the American Chemical Society*, *57*(12), 2680–2684. https://doi.org/10.1021/ja01315a102

Rahm, L., Håkansson, B., Larsson, P., Fogelqvist, E., Bremle, G., & Valderrama, J. (1995). Nutrient and persistent pollutant deposition on the Bothnian Bay ice and snow fields. *Water Air and Soil Pollution*, *84*, 187–201. https://doi.org/10.1007/bf00479597

Roukaerts, A., Deman, F., Linden, F. V., Carnat, G., Bratkic, A., Moreau, S., et al. (2021). The biogeochemical role of a microbial biofilm in sea ice: Antarctic landfast sea ice as a case study. *Elementa: Science of the Anthropocene*, *9*(1), 00134. https://doi.org/10.1525/elementa.2020.00134

Rysgaard, S., & Glud, R. N. (2004). Anaerobic N_2 production in Arctic sea ice. *Limnology & Oceanography*, *49*, 86–94. https://doi.org/10.4319/lo.2004.49.1.0086

Rysgaard, S., Glud, R. N., Sejr, M. K., Blicher, M. E., & Stahl, H. J. (2008). Denitrification activity and oxgen dynamics in Arctic sea ice. *Polar Biology*, *31*, 527–537. https://doi.org/10.1007/s00300-007-0384-x

Saenz, B. T., & Arrigo, K. R. (2014). Annual primary production in Antarctic sea ice during 2005–2006 from a sea ice state estimate. *Journal of Geophysical Research: Oceans*, *119*, 3645–3678. https://doi.org/10.1002/2013JC009677

Schnack-Schiel, B., Thomas, D. N., Haas, C., Dieckmann, G. S., & Alheit, R. (2001). The occurrence of the copepods Stephos longipes (Calanoida) and Drescheriella glacialis (Harpacticoida) in summer sea ice in the Weddell Sea, Antarctica. *Antarctic Science*, *13*(2), 150–157. https://doi.org/10.1017/s0954102001000232

Sturm, M., & Massom, R. A. (2017). In D. N. Thomas, & G. S. Dieckmann (Eds.), *Snow and sea ice*. (2nd ed., pp. 153–204). Wiley-Blackwell. https://doi.org/10.1002/9781444317145.ch5

Suzuki, R., & Ishimaru, T. (1990). An improved method for the determination of phytoplankton chlorophyll using N, N-dimethylformamide. *Journal of the Oceanographic Society of Japan*, *46*, 190–194. https://doi.org/10.1007/BF02125580

Thomas, D. N., & Dieckmann, G. S. (2002). Biogeochemistry of Antarctic sea ice. In R. N. Gibson, M. Barnes, & R. J. A. E. Atkinson (Eds.), *Oceanography and marine Biology: An annual Review* (Vol. 40, pp. 43–169). CRC Press.

Thomas, D. N., Lara, R. J., Eicken, H., Kattner, G., & Skoog, A. (1995). Dissolved organic matter in Arctic multi-year sea ice during winter: Major components and relationship to ice characteristics. *Polar Biology*, *15*(7), 477–483. https://doi.org/10.1007/bf00237461

Toyota, T., Massom, R., Lecimte, O., Nomura, D., Heil, P., Tamura, T., & Fraser, A. D. (2016). On the extraordinary snow on the sea ice off East Antarctica in late winter, 2012. *Deep-Sea Research II*, *131*(2016), 53–67. https://doi.org/10.1016/j.dsr2.2016.02.003

Tréguer, P. J., & De La Rocha, C. L. (2013). The World Ocean silica cycle. *Annual Review of Marine Science*, *5*, 477–501. https://doi.org/10.1146/annurev-marine-121211-172346

Ushio, S. (2006). Factors affecting fast-ice break-up frequency in Lützow-Holm Bay, Antarctica. *Annals of Glaciology*, *44*, 177–182. https://doi.org/10.3189/172756406781811835

Vancoppenolle, M., Goosse, H., de Montety, A., Fichefet, T., Tremblay, B., & Tison, J.-L. (2010). Modeling brine and nutrient dynamics in Antarctic sea ice: The case of dissolved silica. *Journal of Geophysical Resesearch: Oceans*, *115*, C02005. https://doi.org/10.1029/2009JC005369

WMO. (2014). *WMO sea ice nomenclature*. World Meteorological Organisation.

Wongpan, P., Meiners, K. M., Langhorne, P. J., Heil, P., Smith, I. J., Leonard, G. H., et al. (2018). Estimation of Antarctic land-fast sea ice algal biomass and snow thickness from under-ice radiance spectra in two contrasting areas. *Journal of Geophysical Research: Oceans*, *123*(3), 1907–1923. https://doi.org/10.1002/2017jc013711